

IMMUNOLOGY

Inflammasome activation and IL-1 signaling during placental malaria induce poor pregnancy outcomes

Aramys S. Reis^{1,2}, Renato Barboza³, Oscar Murillo¹, André Barateiro¹, Erika P. M. Peixoto¹, Flávia A. Lima¹, Vinícius M. Gomes⁴, Jamille G. Dombrowski¹, Vinícius N. C. Leal⁵, Franciele Araujo⁶, Carla L. Bandeira¹, Rosana B. D. Araujo¹, Rita Neres⁷, Rodrigo M. Souza^{1,8}, Fabio T. M. Costa⁹, Alessandra Pontillo⁵, Estela Bevilacqua⁶, Carsten Wrenger¹, Gerhard Wunderlich¹, Giuseppe Palmisano¹, Leticia Labriola⁴, Karina R. Bortoluci³, Carlos Penha-Gonçalves⁷, Lígia A. Gonçalves¹, Sabrina Epiphany¹⁰, Claudio R. F. Marinho^{1*}

Copyright © 2020
The Authors, some
rights reserved;
exclusive licensee
American Association
for the Advancement
of Science. No claim to
original U.S. Government
Works. Distributed
under a Creative
Commons Attribution
NonCommercial
License 4.0 (CC BY-NC).

Placental malaria (PM) is associated with severe inflammation leading to abortion, preterm delivery, and intrauterine growth restriction. Innate immunity responses play critical roles, but the mechanisms underlying placental immunopathology are still unclear. Here, we investigated the role of inflammasome activation in PM by scrutinizing human placenta samples from an endemic area and ablating inflammasome components in a PM mouse model. The reduction in birth weight in babies from infected mothers is paralleled by increased placental expression of AIM2 and NLRP3 inflammasomes. Using genetic dissection, we reveal that inflammasome activation pathways are involved in the production and detrimental action of interleukin-1 β (IL-1 β) in the infected placenta. The IL-1R pharmacological antagonist Anakinra improved pregnancy outcomes by restoring fetal growth and reducing resorption in an experimental model. These findings unveil that IL-1 β -mediated signaling is a determinant of PM pathogenesis, suggesting that IL-1R antagonists can improve clinical outcomes of malaria infection in pregnancy.

INTRODUCTION

Plasmodium infection in pregnant women is a major cause of maternal illness and a threat to neonatal health in malaria-endemic areas. The accumulation of infected red blood cells (iRBCs) in the placenta induces severe local inflammation deregulating placental physiology and tissue morphology (1). These alterations impair local maternal blood supply, hormonal levels, and maternal-fetal exchanges, leading to poor pregnancy outcomes such as abortion, preterm delivery, intrauterine growth retardation (IUGR), and low birth weight (LBW) (2).

The placenta represents an immunologic barrier against microbial infection that protects the fetus while ensuring its proper development (3). Both the maternal immune system and fetal-derived trophoblast cells are capable of recognizing and responding to pathogens via innate immunity sensors (4, 5). Several innate receptors are known to recognize malaria parasite-derived products, inducing local inflammation. Namely, the plasmodial glycosylphosphatidylinositol (GPI) binds to Toll-like receptor 2 (TLR2) and TLR4 (6), whereas the DNA-hemozoin complex binds to TLR9 (7), leading to the production of tumor necrosis factor- α (TNF- α), interferon- γ (IFN- γ),

and pro-interleukin-1 β (IL-1 β) cytokines (8). We have recently reported that the TLR4/MyD88 pathway has a pivotal role in the disease pathogenesis, inducing pro-IL-1 β production and expression of the intracellular sensors absent in melanoma 2 (AIM2), NOD-, LRR- and pyrin domain-containing protein 3 (NLRP3), and NLR family CARD domain-containing 4 (NLRC4) (9–11). The activation of these sensors is directly linked to the formation of inflammasomes (12), multiprotein complexes responsible for the activation of caspase-1, which leads to the maturation and secretion of IL-1 β (13). Current findings have shown that both hemozoin, a by-product of *Plasmodium*-iRBCs metabolism, and *Plasmodium* DNA are capable of activating NLRP3 (14) and AIM2 (15), respectively. However, the contribution of inflammasomes to placental malaria (PM) pathogenesis remains unclear. In vitro studies have suggested that IL-1 β -dependent NLRP3 activation by uric acid may be associated with progression to preeclampsia (16). Consistent with these studies, increased IL-1 β circulating levels have been correlated with abortion in experimental murine models of the disease (17) and with LBW in newborns from pregnant women with PM (18). In this context, pharmacological inhibition of the IL-1 axis using biopharmaceuticals offers new prospects to treat inflammatory diseases during pregnancy (19). One of these promising pharmaceuticals is Anakinra, a recombinant human IL-1 receptor antagonist (IL-1Ra) (20) that has been used to improve the prognosis of complicated pregnancies by reducing inflammation (19). Nevertheless, there are no reports on the inhibition of the IL-1 pathway in PM.

Here, we demonstrate that AIM2 and NLRP3 inflammasomes have a major contribution in triggering PM-associated pathology and that pharmacological intervention with Anakinra improved pregnancy outcomes in experimental PM. These findings warrant further investigation of IL-1 β pharmacological targeting to overcome clinical pregnancy complications due to malaria infection.

¹Departamento de Parasitologia, Instituto de Ciências Biomédicas, Universidade de São Paulo, São Paulo, SP, Brazil. ²Faculdade de Medicina, Centro de Ciências Sociais, Saúde e Tecnologia, Universidade Federal do Maranhão, Imperatriz, MA, Brazil. ³Departamento de Ciências Biológicas, Universidade Federal de São Paulo, Diadema, SP, Brazil. ⁴Departamento de Bioquímica, Instituto de Química, Universidade de São Paulo, São Paulo, SP, Brazil. ⁵Departamento de Imunologia, Instituto de Ciências Biomédicas, Universidade de São Paulo, São Paulo, SP, Brazil. ⁶Departamento de Biologia Celular e do Desenvolvimento, Instituto de Ciências Biomédicas, Universidade de São Paulo, São Paulo, SP, Brazil. ⁷Instituto Gulbenkian de Ciência, Oeiras, Portugal. ⁸Centro Multidisciplinar, Campus Floresta, Universidade Federal do Acre, Cruzeiro do Sul, AC, Brazil. ⁹Departamento de Genética, Evolução e Bioagentes, Instituto de Biologia, Universidade Estadual de Campinas, Campinas, SP, Brazil. ¹⁰Departamento de Análises Clínicas e Toxicológicas, Faculdade de Ciências Farmacêuticas, Universidade de São Paulo, São Paulo, SP, Brazil.

*Corresponding author. Email: marinho@usp.br

RESULTS

Placental *Plasmodium falciparum* infection impairs fetal growth and activates placental caspase-1 and IL-1 β

To understand the immunologic mechanisms, mainly the involvement of inflammasome in the pathogenesis of human PM, we used *P. falciparum*-infected (*Pf*-I) placentas. The relationship between inflammasome activation and PM development was achieved by comparing with noninfected (NI) placentas with similar characteristics (gravidity, maternal, and gestational age), although infected pregnant women had significantly lower blood hemoglobin levels and weight

gain (table S1). Histological analysis of NI placentas (Fig. 1A) presented qualitative differences from the infected placentas, which revealed iRBCs in the intervillous space (IVS), hemozoin deposits, necrotic areas, syncytial nuclear aggregates, and fibrinoid necrosis (Fig. 1, B to G, and table S2). Unlike healthy women, infected pregnant women showed a reduction in newborn (Fig. 1H) and placental (Fig. 1I) weight and an increased number of monocytes (CD68⁺ cells) in the IVS (Fig. 1J). In addition, the levels of IL-1 β , TNF- α , IL-6, and IL-10 cytokines were increased in the infected placentas, even though the placental plasma was collected postpartum (Fig. 1K and table S2).

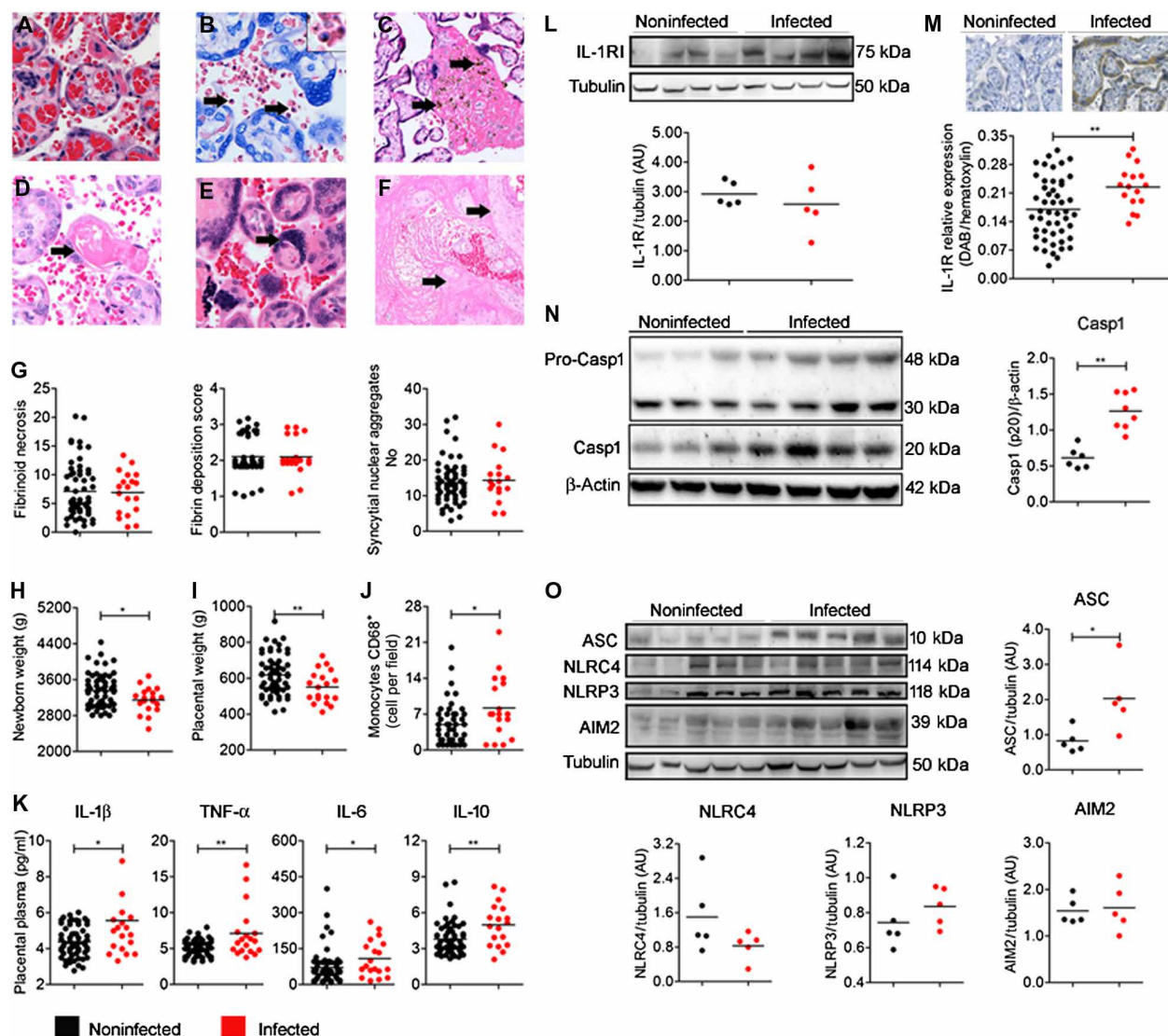


Fig. 1. *Pf* infection during pregnancy induces placental pathology, poor outcomes, and inflammasome activation. (A to F) Representative histology images of placentas collected from NI (A) and *Pf*-I (B to F) women. Black arrows indicate the presence of iRBCs in the IVS (B), hemozoin deposition (C), necrotic villi (D), syncytial nuclear aggregates (E), and fibrinoid necrosis areas (F). AU, arbitrary units; DAB, 3,3'-diaminobenzidine. Tissue imaged with $\times 40$ (A and D to F), $\times 63$ (B), and $\times 20$ (C) magnification. Quantification of the histopathological parameters (G) and newborn (H) and placental (I) weight. (J) Quantification of monocytes within the IVS in 10 different microscopic fields. (K) Placental plasma levels of IL-1 β , TNF- α , IL-6, and IL-10 cytokines measured by CBA. (L and M) Relative expression of placental IL-1R protein measured by Western blot (WB) (L) and immunohistochemistry (M) normalized by a fraction of the area. (N and O) Placental caspase-1 activity (N) and protein expression of AIM2, NLRP3, and NLRC4 receptors, and ASC adaptor (O) identified by WB. WB data were quantified by densitometry and normalized by tubulin (L and O) or β -actin (N). Data are expressed as scatter plot and group mean (dash). Number of individuals: (G to K) NI = 59 and *Pf*-I = 19; (L) NI = 5 and *Pf*-I = 5; (M) NI = 49 and *Pf*-I = 16; (N) NI = 6 and *Pf*-I = 8; and (O) NI = 5 and *Pf*-I = 5. The differences between NI and infected pregnant women were determined by Student's *t* test (H and I) or Mann-Whitney rank sum test (G and J to O). **P* < 0.05 and ***P* < 0.01. (A to F) Photo credit: Rodrigo M. Souza, University of São Paulo.

Parallel to the increased IL-1 β levels, infection also induced IL-1R overexpression in the placenta, as shown by immunohistochemistry (Fig. 1M). Likewise, infection led to the increase in caspase-1 (p20 subunit) processing in placental tissue (Fig. 1N), indicating that this enzyme is actively participating in the IL-1 β biogenesis. Infected placentas displayed an increase in the apoptosis-associated speck-like protein containing a C-terminal caspase recruitment domain (ASC) adaptor protein levels (Fig. 1O), suggesting that placental inflammation induced by *Pf* infection is linked to increased inflammasome activity. Moreover, a Spearman's rank-order correlation coefficient (r_s) analysis evidenced strong negative correlations between the placental weight and IL-1 β , TNF- α , and caspase-1, as well as between newborn length and AIM2 and ASC (fig. S1). Together, these results strengthen the role of the IL-1 axis in the pathogenesis of malaria in pregnancy.

Pf-iRBCs induce IL-1 β secretion in human monocytes and trophoblast cells

Monocytes and trophoblasts are known to express inflammasome components, which result in IL-1 β secretion in response to different stimuli (16, 21). Therefore, we evaluated caspase-1 activity and consequent IL-1 β release in THP-1 (human monocytic cell line) and BeWo (human trophoblastic choriocarcinoma cell line) cells stimulated with extracts of *Pf*-iRBCs or NI RBCs. We detected that the iRBC extract induced activation of caspase-1 in THP-1 (Fig. 2A) and BeWo (Fig. 2C) cells when compared with negative controls and that this stimulation promoted the secretion of IL-1 β in a dose-dependent manner (Fig. 2, B and D). Furthermore, similar experiments were performed in primary cultures of human monocytes and trophoblasts where iRBC stimulation also led to IL-1 β secretion in a dose-dependent manner (Fig. 2, E and F), corroborating the results obtained in the cell lines. Together, these data indicate a relation between caspase-1 activation and the secretion of IL-1 β in response to *Pf* infection.

Murine placental *Plasmodium berghei* infection induces IL-1 β production

We used a PM experimental model to ascertain whether IL-1 β and the inflammasome activity are involved in the PM pathogenesis (9, 22). On gestational day 13 (G13), C57BL/6 pregnant mice were infected with *P. berghei* (*Pb*) NK65^{GFP}. Consistent with previous studies, at G19, infected pregnant mice that displayed PM presented a reduction in placental vascular spaces (Fig. 3A) and fetal weight (Fig. 3B) and a tendency for augmented fetal resorption rate (Fig. 3C) when compared with NI controls (9, 22). The increased levels of proinflammatory cytokines such as IL-1 β , TNF- α , IFN- γ , and IL-6 in placental tissue (Fig. 3D) and plasma, except IL-1 β (Fig. 3E), of infected females paralleled the profile we found in *Pf*-I human placentas (Fig. 1K). However, IL-10 secretion was unaltered in infected mice (Fig. 3, D and E). Despite the fact that IL-1 β was not detected in the plasma of any group, probably due to its short plasma half-life and restriction to tissues (23), analysis showed that *Pb* infection led to an increase in placental IL-1 β (Fig. 3D) and caspase-1 (p20 subunit) (Fig. 3F) levels. These results underline that in analogy with the human infection, IL-1 β takes part in placental inflammation in murine PM.

AIM2 and NLRP3 inflammasomes impair fetal growth in pregnant mice with PM

To evaluate the contribution of inflammasomes to PM pathogenesis, we made use of gene-deficient mice for relevant inflammasome components. We found that the fetal weight of *Casp1/11*^{-/-}, *Asc*^{-/-},

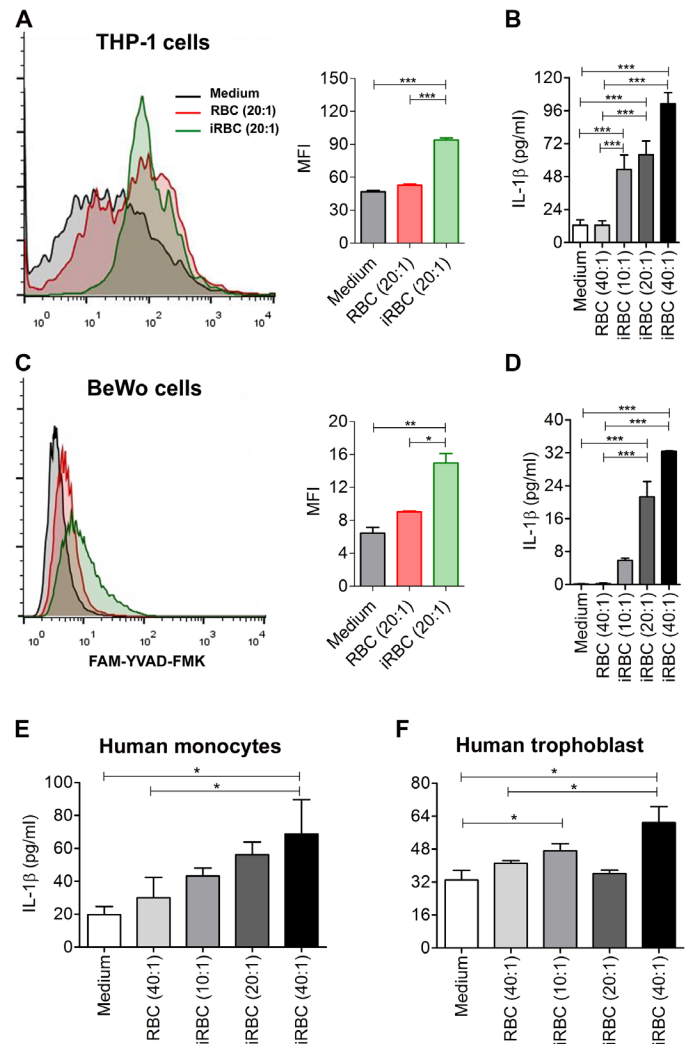


Fig. 2. IL-1 β production in human monocytes and trophoblasts exposed to *Pf*-iRBCs. (A and C) Flow cytometry histograms and column bar graph of the caspase-1 median fluorescence intensity (MFI) of THP-1 monocytic (A) and BeWo trophoblast (C) cell lines, stimulated with an extract of *Pf*-I (iRBCs, green) or NI (RBCs, red) RBCs for a 12-hour period in a 20:1 RBCs:cell ratio. THP-1 cells were prestimulated with 100 nM lipopolysaccharide. Medium was added to the nonstimulated control group (gray histogram). (B and D to F) Secreted IL-1 β was evaluated in the supernatant of THP-1 (B) and BeWo (D) cells, as well as in primary cultures of human monocytes (E) and trophoblasts (F) stimulated with an extract of RBCs (ratio, 40:1) and iRBCs at different ratios (10:1, 20:1, and 40:1) for 24 (E) or 48 hours (B, D, and F). Data are represented as means \pm SD of triplicate cultures that were performed in two (A, C, E, and F) and three (B and D) independent experiments. The differences between each group were determined by one-way ANOVA with Bonferroni's post hoc correction. * P < 0.05, ** P < 0.01, and *** P < 0.001.

Nlrp3^{-/-}, and *Aim2*^{-/-} progenies was only marginally affected by infection when compared with C57BL/6 wild-type (WT) mice (Fig. 4A). On the other hand, fetal weight reduction was prominent in the *Nlrp3*^{-/-} progenies, albeit somewhat lower than WT (Fig. 4A). Similarly, fetal resorption induced by infection was not affected in the absence of *Nlrp3* or *Nlrp3* but followed the fetal weight trend for the reduction observed in *Casp1/11*^{-/-}, *Asc*^{-/-}, and *Aim2*^{-/-} pregnant mice (Fig. 4B), although without statistical significance. These results indicate that the activation of the NLRP3–AIM2–caspase-1 axis affects fetal growth

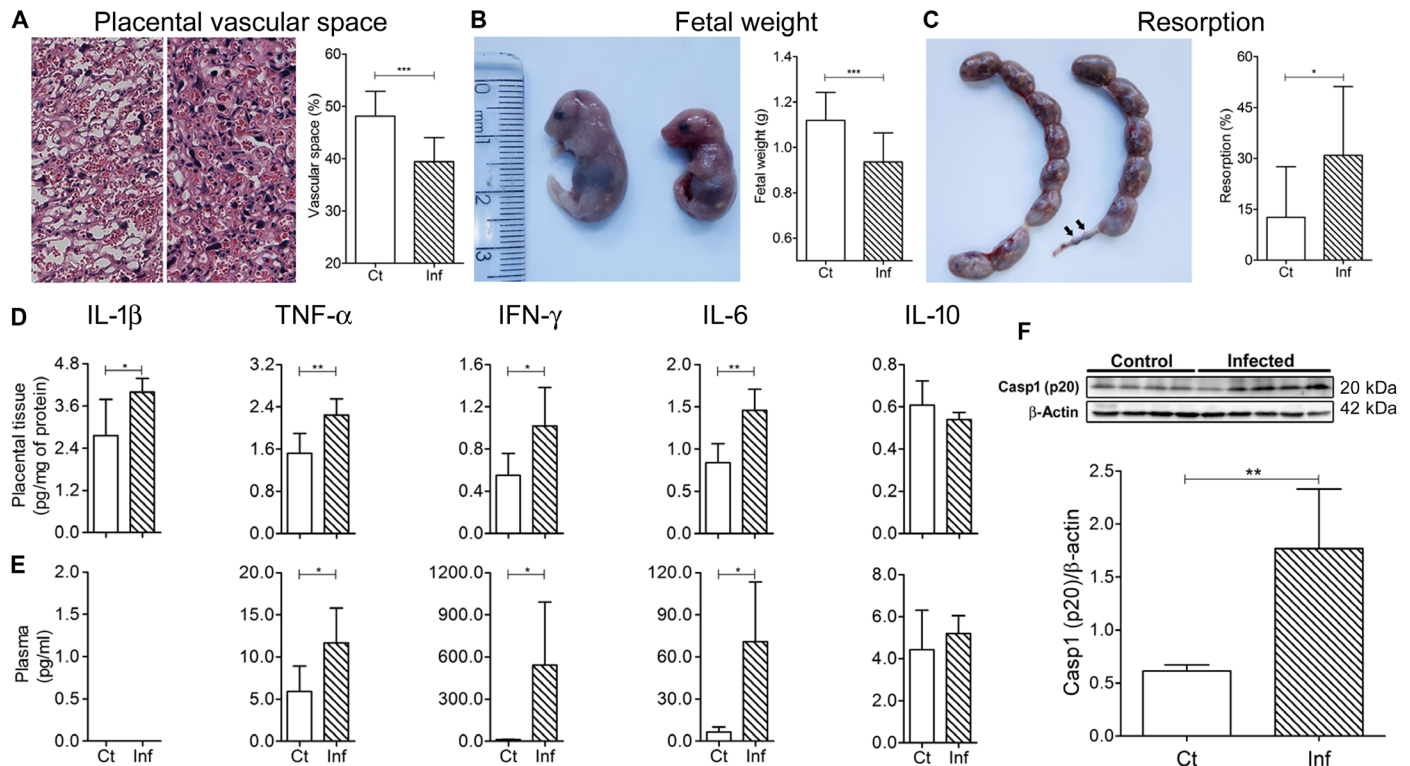


Fig. 3. *Pb* infection during murine pregnancy induces placental pathology and caspase-1 activation. (A to C) Images illustrated the NI (Ct, left) and infected (Inf, right) placental vascular spaces (A), fetus (B), and uterus (C) of mice. (A) Relative quantification of placental vascular space. (B) Fetal weight measured at G19. (C) Relative quantification of the resorption number (arrows) in relation to the total fetuses' number (viable and resorptions). (D and E) Protein levels of IL-1 β [enzyme-linked immunosorbent assay (ELISA)], TNF- α , IFN- γ , IL-6, and IL-10 (CBA) in placentas (D) and plasma (E) collected from NI (Ct) or infected (Inf) mice. (F) Placental caspase-1 (p20) activity by WB in NI (Ct) or infected (Inf) mice, normalized by β -actin. Data are represented as means \pm SD of 29 to 49 placentas or fetuses ($n = 8$ to 12 pregnant mice) (A and B) and 5 to 12 pregnant mice (C to F) per group, which were performed in two or more independent experiments. The differences between the control group (Ct) and infected (Inf) pregnant mice were determined by Student's *t* test. * $P < 0.05$, ** $P < 0.01$, and *** $P < 0.001$. (A to C) Photo credit: Aramys S. Reis, University of São Paulo.

and viability during murine PM. Accordingly, we noted that IL-1 β production in the placental tissue was not affected by infection in pregnant mice deficient in *Casp1/11*^{-/-}, *Asc*^{-/-}, *Nlrp3*^{-/-}, and *Aim2*^{-/-}, in contrast with WT mice (Fig. 4C). Conversely, IL-1 β production in placentas collected from *Nlr4*^{-/-} mice was increased by infection, suggesting that this inflammasome molecule is not involved in the induction of IL-1 β production during murine PM. This result matches the data obtained from human placentas, because no differential expression of NLRC4 was detected upon infection (Fig. 1K).

Pregnancy increased the susceptibility to *Pb* expansion in pregnant mice irrespective of genetic ablation of *Casp1/11*, *Asc*, *Nlr4*, and *Nlrp3* (fig. S2), indicating that the role of the inflammasome components involved in placental inflammatory responses and poor pregnancy outcomes do not act through controlling peripheral parasite burden. However, parasitemia measured in *Aim2*^{-/-}-infected mice was reduced in comparison to the other mouse strains (fig. S2), suggesting that this receptor may contribute to a host response that favors parasite expansion. These observations indicate that AIM2 and, possibly, NLRP3 inflammasomes contribute to PM pathogenesis and are tightly linked with fetal growth restriction and placental IL-1 β production.

IL-1 axis activation impairs pregnancy outcomes that are reverted by pharmacological intervention

To establish whether IL-1 β production is determinant for PM development and poor fetal outcomes, we modulated the IL-1 axis

signaling by using mice deficient in *Il1b* and *Il1*-receptor (*Il1r1*) or blocking the WT IL-1R with Anakinra, a recombinant of the IL-1Ra (12). Our results showed that in the absence of IL-1 β signaling, either by genetic ablation or by blocking the receptor, the fetal weight in infected mice was highly improved (relative weight reduction, 3.7% for *Il1b*^{-/-} and 1.1% for *Il1r1*^{-/-} versus 16.4% for WT and 0.4% for Anakinra versus 11.8% for vehicle) (Fig. 5, A and B). In addition, the absence of IL-1 β signaling reduced the resorption rate in relation to WT or vehicle, but there was no difference between the manipulated groups (0.7 for *Il1b*^{-/-} and 0.5 for *Il1r1*^{-/-} versus 2.5 for WT and 0.5 for Anakinra versus 1.9 for vehicle) (Fig. 5, C and D). These observations indicate that IL-1 β signaling significantly contributes to impair fetal growth and viability in pregnant mice with PM. It is known that one of the main causes of fetal growth restriction in PM is the dysregulation of nutrient transporters. Therefore, to ascertain the interference of IL-1 β signaling in the nutrient transporters *Slc38a1* (SNAT1), *Slc38a2* (SNAT2), and *Slc2a1* (GLUT1), the gene expression was evaluated. Expectedly, we observed that placentas collected from WT mice with PM presented reduced mRNA levels of all three transporters (fig. S3). This phenomenon was not observed in infected placentas collected from *Il1r*^{-/-} or *Il1b*^{-/-} mice or infected pregnant mice treated with Anakinra. These findings suggest that propagation of IL-1 β signaling plays a role in the regulation of amino acid and nutrient transporters, which may explain the poor pregnancy outcomes associated with PM.

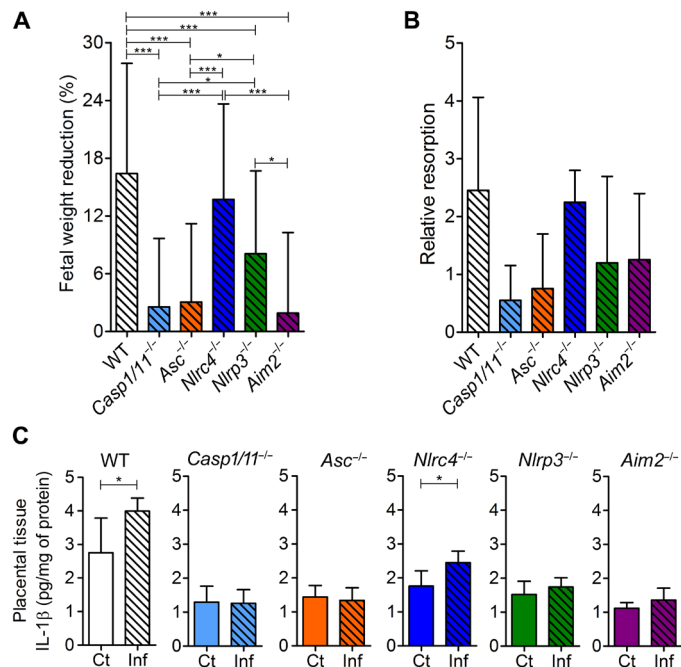


Fig. 4. AIM2 and NLRP3 inflammasomes are associated with poor pregnancy outcomes in *Pb*-infected mice. Evaluation of pregnancy outcomes in mice deficient for *Casp1/11*, *Asc*, *Nlrp3*, and *Aim2* genes of the inflammasome complexes. (A) Percentage of weight reduction of fetuses born from infected pregnant mice in relation to their NI controls at G19. (B) Relative resorption rates of infected in relation to their NI controls. (C) Measure of IL-1 β levels in placentas collected from infected (Inf) and NI (Ct) mice by ELISA. Pooled placenta samples, each containing four mouse placentas per sample, were used for protein extraction. WT refers to C57BL/6 mice. Data are represented as means \pm SD of 37 to 39 fetuses ($n = 5$ to 14 pregnant mice) (A) and 5 to 14 pregnant mice (B and C) per group, which were performed in two or more independent experiments. The differences between each group were determined by one-way ANOVA with Bonferroni's post hoc correction (A and B) and Student's *t* test (C). * $P < 0.05$ and *** $P < 0.001$.

Notwithstanding, the absence of IL-1 β signaling restrains the increase in parasitemia when compared with the WT control (fig. S4), suggesting that besides its role in PM pathogenesis, the IL-1 axis may also take part in the parasite controlling responses in pregnant mice. Moreover, in line with previous findings (9–11), the MyD88 protein was shown to be critical for the poor fetal outcomes and IL-1 β production (fig. S5). Besides being an important TLR adaptor molecule, MyD88 is also essential for IL-1R signaling, thereby contributing to both the synthesis and the effector response of IL-1 β . Together, our results open new perspectives for the role of the IL-1 axis signaling in placental malaria pathogenesis, which can be reverted by pharmacologically blocking the receptor.

DISCUSSION

It is well established that malaria during pregnancy increases the risk of adverse fetal outcomes, such as abortion, IUGR, premature birth, and LBW. Here, we present findings that add to the argument for an understanding of placental malaria pathogenesis. We report that impaired fetal growth is associated with IL-1 β production in human and murine PM and that the AIM2/NLRP3 inflammasome is critical to produce IL-1 β in the infected placenta that, in turn,

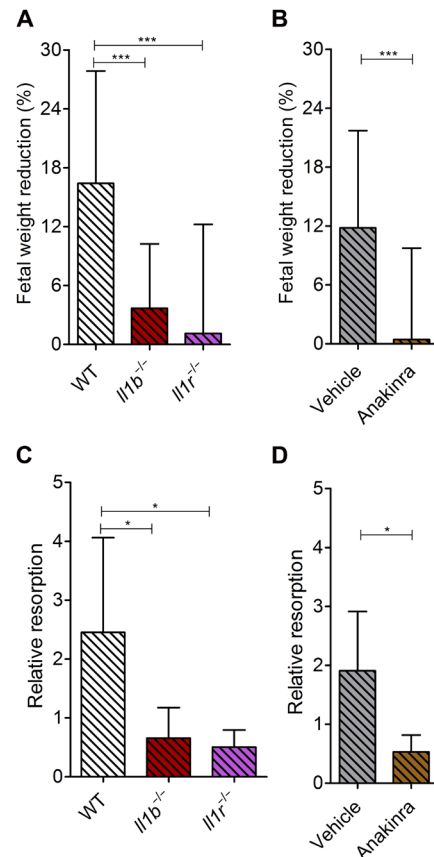


Fig. 5. Impaired pregnancy outcomes are reverted by IL-1 axis genetic ablation and pharmacological blocking. Assessment of IL-1 β signaling impact in fetal by genetic ablation of *Il1b* and *Il1r1* or by blocking the receptor with Anakinra, a recombinant of the IL-1Ra. (A and B) Weight reduction of fetuses born from infected pregnant mice expressed in percentage of their NI controls at G19. (C and D) Relative resorption rates of infected in relation to their NI controls. (B and D) Anakinra treatment was performed in WT (C57BL/6) mice, and vehicle represents an infected group treated with Anakinra denaturated in phosphate-buffered saline. Data are represented as means \pm SD of 24 to 46 fetuses ($n = 3$ to 12 pregnant mice) (A and C) or 3 to 12 pregnant mice (B and D) per group and are cumulative of two or more independent experiments. The differences between each group were determined by one-way ANOVA with Bonferroni's post hoc correction (A and C) or Student's *t* test (B and D). * $P < 0.05$ and *** $P < 0.001$.

impacts the normal course of pregnancy in infected females. We demonstrate that genetic ablation and pharmacological inhibition of IL-1 β signaling reverted poor pregnancy outcomes of placental malaria.

Placental inflammation is a critical pathological event underlying pregnancy impairment in *Pf*-I mothers (1). Increased placental levels of proinflammatory mediators, including IL-1 β and TNF- α , are frequently associated with IUGR in pregnant women infected with *Pf* (24). In line with these findings, we show that caspase-1 activation and IL-1 β production in the placenta were consistent with placental tissue alterations and reduced birth weight in women infected with *Pf* during pregnancy. These events suggest that the proinflammatory response leading to IL-1 β production is a determinant of placental malaria severity. Noticeably, pharmacological inhibition of IL-1 β signaling conferred protection from pregnancy impairments in infected mice, unveiling deleterious effects of IL-1 β action on the developing

fetus. Our findings provide a molecular link of placental inflammation with reduced birth weight and increased fetal resorption rate in infected mice. Accordingly, proinflammatory cytokines have been implicated in spontaneous abortions in women (25) and with increased abortion rates in PM murine models (17, 26), possibly due to their high toxicity to the embryos (27).

In murine malaria models, $\text{TNF-}\alpha$, $\text{IFN-}\gamma$, and $\text{IL-1}\beta$ production is frequently linked to the TLR/MyD88 pathway activation (6, 28), and a similar molecular mechanism is also operating in murine PM (9–11). It should be noted that besides MyD88 activation, caspase-1 activity is also critical for the complete maturation and secretion of $\text{IL-1}\beta$, which depends on inflammasome formation (29). Here, we show that the central role of $\text{IL-1}\beta$ in affecting fetal growth in experimental PM is dependent on AIM2 and, to a lesser extent, on NLRP3 inflammasome formation. Furthermore, caspase-1 activation and $\text{IL-1}\beta$ secretion in monocytes and trophoblasts, cell lines, and primary cells, stimulated with *Pf*-iRBCs, suggest a possible contribution of these cells to innate immune responses during PM pathogenesis. Both cell types have receptors linked to innate immunity capable of recognizing

parasite by-products that consequently lead to proinflammatory cytokine production, including $\text{IL-1}\beta$ (16, 30, 31).

It is well established that *Pf* double-stranded DNA (dsDNA) and hemozoin can activate AIM2 and NLRP3, respectively, leading to inflammasome formation and caspase-1 activation (15). Those by-products of *Plasmodium* infection are released at the end of the blood schizogony and trigger $\text{IL-1}\beta$ production (14, 15). In particular, parasite DNA is known to be a potent AIM2 inflammasome activator, even at low concentrations (15). Although placental damage in experimental PM is associated with accumulation of low amounts of iRBCs (9, 22), it is plausible that AIM2 substantially contributes to local inflammation and induction of subsequent pregnancy complications. On the other hand, NLRP3-mediated inflammation is dependent on high hemozoin concentrations (14, 15). The reduced accumulation of placental hemozoin in our experimental mouse model due to the short period of infection (9) may explain the lower contribution of this receptor to $\text{IL-1}\beta$ production and fetal weight reduction.

Nevertheless, the NLRP3 inflammasome is essential in other pregnancy-related complications. A model of pregnancy failure

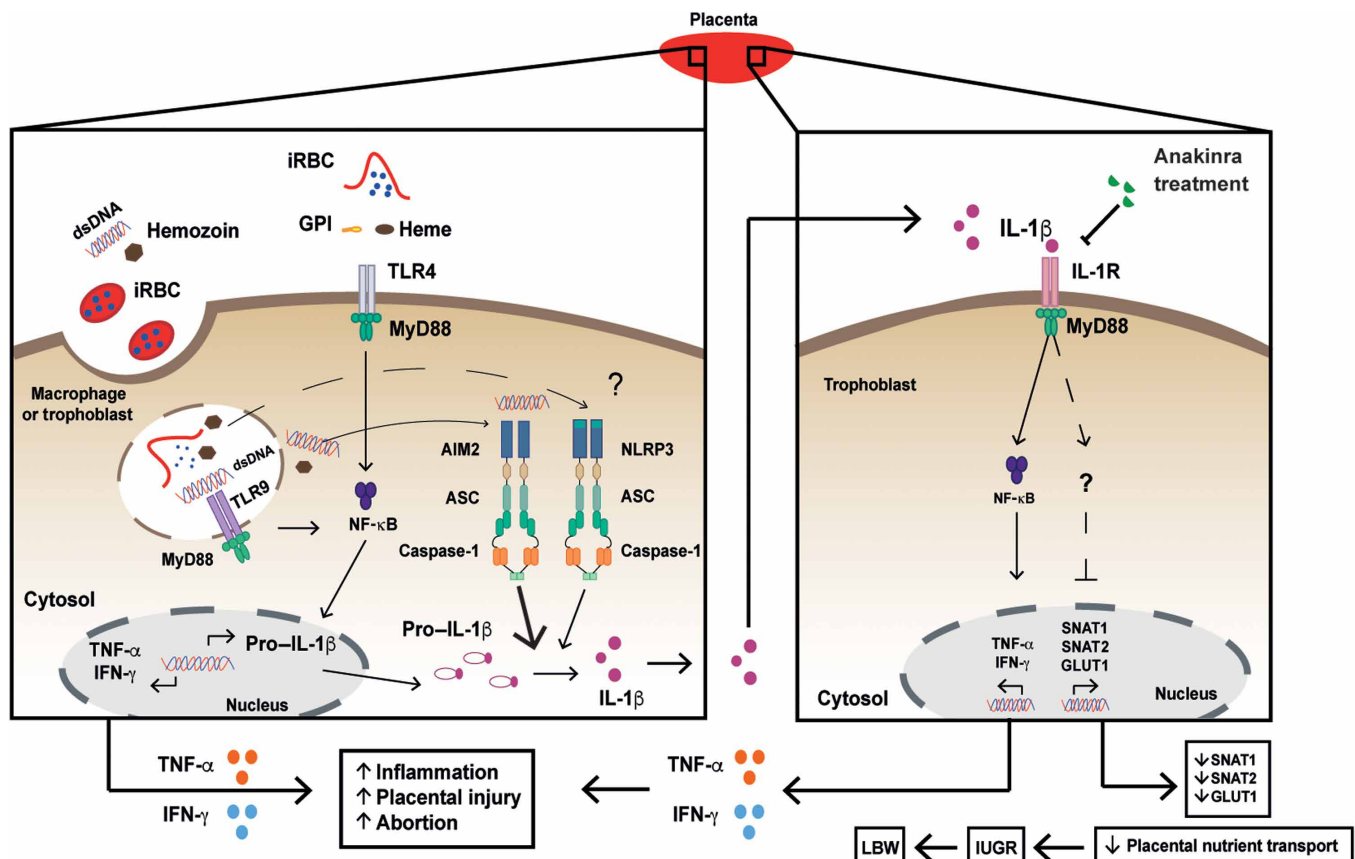


Fig. 6. Proposed mechanism of inflammasome activation during placental malaria. *Plasmodium* antigens and cellular danger signals like GPI, hemozoin, dsDNA, and heme are recognized by TLR4 and TLR9 expressed in placental macrophages and trophoblasts. This phenomenon triggers these pathways through MyD88, activating the nuclear factor κB (NF- κB) transcription factor, which induces transcription of proinflammatory cytokines such as $\text{TNF-}\alpha$, $\text{IFN-}\gamma$, and pro- $\text{IL-1}\beta$. In addition, hemozoin and dsDNA activate NLRP3 and AIM2 inflammasomes, respectively, which induce pro- $\text{IL-1}\beta$ cleavage by caspase-1, which ultimately will be secreted in its active form. Active $\text{IL-1}\beta$ will bind, with high affinity, to its receptor (IL-1R), triggering the downstream events that sustain the production of more proinflammatory cytokines and, possibly, impairing the expression and function of nutrient transporters, such as SNAT1, SNAT2, and GLUT1. Dysregulation of nutrient transportation will promote IUGR, consequently leading to poor pregnancy outcomes such as LBW. Furthermore, increasing levels of $\text{IL-1}\beta$, $\text{TNF-}\alpha$, and $\text{IFN-}\gamma$ in the placenta also contribute to local inflammation, causing severe damage in placental tissue and poor pregnancy outcomes. The archetype of placental malaria, reduced fetal development, can be reverted in our experimental model with Anakinra treatment, a recombinant of the IL-1Ra . PAMPs, pathogen-associated molecular patterns; DAMPs, damage-associated molecular patterns.

induced by *Listeria monocytogenes* showed that reduced survival rates of embryos were only dependent on NLRP3 activation (32). These findings were paralleled by increased levels of systemic IL-1 β , which induced TNF- α , monocyte chemoattractant protein 1 (MCP-1), IL-6, and IL-8 production by murine trophoblasts (32). Therefore, we propose that AIM2- and NLRP3-dependent IL-1 β production has a pivotal role in the molecular mechanisms, propagating placental inflammation and compromising fetal growth and fetal survival.

We observed that placentas of pregnant women infected with *Pf* displayed increased levels of IL-1R, which can potentiate the downstream effect of IL-1 β . Notably, and differently from WT mice, pregnant *Il1b*^{-/-} and *Il1r1*^{-/-} mice infected with *Pb* lack poor fetal outcomes, reinforcing the role of the IL-1 signaling pathway in the PM pathogenesis. Corroborating human studies (18, 33), our findings suggest that the presence of IL-1 β signaling leads to the diminished expression of nutrient transporters. These transporters are fundamental for nutrient exchanges at the maternal-fetal interface, and dysregulation of their function or expression may compromise the developing fetus. Moreover, our observations in *Il1b*^{-/-} and *Il1r1*^{-/-} pregnant mice did not show alterations in fetal nurturing, suggesting that the IL-1 β signaling pathway may be implicated in the placental nutrient transport impairment in PM (Fig. 6).

The pharmacologic inhibition of IL-1R with Anakinra protected pregnant mice from PM by reverting the fetal growth restriction, confirming the involvement of IL-1 β signaling in the molecular pathogenesis of PM. It is important to highlight that this drug per se did not present any toxicity effects either to the fetuses or to pregnant females in our experimental model. Besides, it is an approved drug to be used in humans that have been used in the treatment of other inflammatory diseases associated with pregnancy, supporting its low toxicity for the females and the growing fetus (19). Together, these observations reinforce the potential of this therapeutic approach, which may be used as an adjunctive treatment to antimalarials for placental inflammatory complications in *Plasmodium* infections. In this context, further studies should be performed to investigate new therapeutic strategies involving the IL-1 β pathway in the treatment of human PM.

MATERIALS AND METHODS

Participants and specimens

NI pregnant women ($n = 59$) and women with a positive molecular diagnosis for *Pf* at the moment of delivery performed by cesarean section (C-section) (active infection) ($n = 19$) were recruited between 2012 and 2014 from a prospective cohort study conducted at the Hospital da Mulher e da Criança do Juruá in Cruzeiro do Sul, Acre, Brazil (34), an endemic and low transmission area for malaria. After delivery, newborns' anthropometric measurements were recorded, and maternal peripheral and placental blood was collected for direct malaria diagnosis, plasma collection, and evaluation of hematologic parameters. Placentas were weighed, and tissue samples were collected, fixed in 10% buffered formalin, and adequately stored until processing (34). In addition, relevant clinical information including maternal and gestational age and gravidity was recorded through structured questionnaires. Infection was confirmed, and *Plasmodium* species was identified using photo-induced electron transfer–polymerase chain reaction (PET-PCR) (35).

All pregnant women who enrolled in the study received the treatment recommended by the Brazilian Ministry of Health after malaria

diagnosis (36) and immediate collection of biological samples. This study was approved by the committees for research of the University of São Paulo and the Federal University of Acre (Plataforma Brasil, CAAE: 03930812.8.0000.5467 and 03930812.8.3001.5010, respectively), according to resolution no. 466/12 of the Brazilian National Health Committee. All the study participants or their legal guardians (if minors) gave written informed consent.

Histopathologic and immunohistochemistry analyses of human placentas

After sample processing, tissue was embedded in paraffin. Placenta sections 5 μ m thick were obtained and mounted on slides using the tissue microarray technique (37). Then, samples were stained with hematoxylin and eosin (H&E) and Giemsa for the histopathologic examination using a Zeiss Axio Imager M2 light microscope equipped with a Zeiss AxioCam HR camera to capture images of placental tissue. Two well-trained pathologists carried out the analysis independently and blindly. When discrepancies were detected between readouts, a reevaluation was conducted, and a decision was established by consensus. Both qualitative and quantitative analyses were performed to evaluate the presence of infected iRBCs in the IVS, hemozoin deposition, syncytial nuclear aggregates, and necrosis in placental tissue (38). For immunohistochemistry, tissue sections were removed from paraffin and rehydrated following antigen retrieval using tris/EDTA (0.01 M/0.001 M, pH 9.0) in the pressurized pan. Endogenous peroxidase was blocked with hydrogen peroxide 1% (v/v), and unspecific binding was avoided using a protein blocking solution. Sections were incubated with anti-CD68 (145M.96; Rocklin, USA) antibody for monocyte identification or anti-IL-1RI (ab106278; Abcam, UK) antibody. Incubations were done overnight at 4°C in a humidified chamber. Samples were then incubated with a secondary antibody conjugated to a horseradish peroxidase (HRP), followed by incubation with 3,3'-diaminobenzidine (DAB) inducing a colorimetric reaction. Last, histologic sections were counterstained with Harris hematoxylin and dehydrated, and slides were sealed with mounting medium. As a positive control, we used a histologic section of the spleen, kidney, and liver, and as a negative control, human placenta sections in which incubation with the primary antibody was substituted by phosphate-buffered saline (PBS). For the analysis of monocyte infiltrates in the IVS, 10 fields were counted with cells stained with the anti-CD68 antibody. For the analysis of relative IL-1R expression, we used ImageJ software (<https://imagej.nih.gov/ij/>). A fraction of the areas stained with DAB (anti-IL-1R) and Harris hematoxylin was quantified, followed by the calculation of the relation between the two stainings.

Trophoblast and monocyte cell line activation assay

Pf NF54-iRBCs were submitted to synchronization in plasma gel (6% Voluven, Fresenius Kabi), purified with a magnetic column (Miltenyi Biotec), counted, and submitted to 10 freeze-thaw cycles to generate the cell lysate. NI RBCs were quantified and submitted to the same lysis process. For the activation assay, we used BeWo, a cell line of trophoblasts derived from human choriocarcinoma, and THP-1, a human cell line of leukemic monocytes. Initially, to promote cell spreading and adhesion, BeWo and THP-1 cells (1×10^5 cells per well) were cultured in 24-well plates and incubated with 1 ml of RPMI 1640 medium (Gibco, USA) supplemented with penicillin (100 U/ml), streptomycin (100 μ g/ml), amphotericin B (2.5 μ g/ml), L-glutamine (2 mM), and fetal bovine serum (FBS) (5%) in a 37°C

atmosphere containing 5% CO₂. In addition, 100 nM phorbol-12 myristate 13-acetate (PMA) was added to THP-1 cultures for 48 hours to induce macrophage differentiation, followed by a prestimulation with lipopolysaccharide (LPS) for 4 hours. Then, cells were exposed (or not) to iRBC or RBC extract in different concentrations for a 12- or 48-hour period. The assays were done in triplicate, and cells were analyzed by flow cytometry for caspase-1 activity and IL-1 β production.

Primary monocyte isolation and stimulation

Mononuclear cells were isolated from 50 ml of peripheral blood of informed healthy female volunteers through Ficoll-Hypaque (GE Healthcare) density gradient. The monocytes were separated from lymphocytes through plastic adherence. Briefly, 4×10^6 mononuclear cells were incubated per well in 24-well culture plates (Corning Costar). After 2 hours, nonadherent cells were removed, while adherent cells (mainly monocytes) were cultured in RPMI 1640 (Gibco, Thermo Fisher Scientific) supplemented with 10% of FBS (Gibco) at 37°C in 5% CO₂ overnight. During the second day, monocytes were primed with LPS (100 ng/ml) from *Escherichia coli* (Sigma-Aldrich, Merck) for 4 hours. After the incubation period, culture medium was replaced, and the cells were stimulated/incubated with RBCs at a ratio of 40:1 (RBCs:monocyte) and iRBCs at a ratio of 10:1, 20:1, and 40:1 for 24 hours. Cell supernatants were collected for cytokine measurements.

Trophoblast cell isolation and differentiation into syncytiotrophoblast

Trophoblast cells were prepared from human term placentas obtained from healthy pregnant women (37 to 39 weeks) upon C-section without complications. The isolation of the trophoblast cells was conducted as described elsewhere (39). Upon cell differentiation, the trophoblasts were primed with LPS (100 ng/ml) from *E. coli* (Sigma-Aldrich, Merck) for 4 hours. After the incubation period, culture medium was replaced, and the cells were stimulated/incubated with RBCs at a ratio of 40:1 (RBCs:trophoblast) and iRBCs at a ratio of 10:1, 20:1, and 40:1 for 48 hours. Cell supernatants were collected for cytokine measurements. Furthermore, cells were plated into six-well (35 mm) multidishes with a 22-mm round cover glass for morphological analysis (39). Briefly, cytokeratin-reactive and multinucleated trophoblast cells were counted to characterize enrichment of the cell culture in trophoblasts cells.

Measuring caspase-1 activity

To measure caspase-1 protease activity, we used a specific fluorescent probe (FAM-YVAD-FMK) that binds to the active form with high affinity. BeWo and THP-1 cells exposed or nonexposed to iRBC or RBC extract, at a ratio of 20:1 (RBCs:cell) by 12-hour period, were stained for 90 min with FAM-YVAD-FMK (Immunochemistry Technologies, USA) as recommended by the manufacturer. Active caspase-1 was measured by flow cytometry. Fluorescent cell data acquisition was done using the FACSCalibur cytometer (BD Biosciences, USA) and analyzed with “FlowJo 10.07r2” software (Treestar, Ashland, USA).

Animals

C57BL/6 WT and *Myd88* (*Myd88*^{−/−}), *Casp1/11* (*Casp1/11*^{−/−}), *Asc* (*Asc*^{−/−}), *Nlrp3* (*Nlrp3*^{−/−}), *Aim2* (*Aim2*^{−/−}), *Nlr4* (*Nlr4*^{−/−}), *Il1b* (*Il1b*^{−/−}), and *Il1r1* (*Il1r1*^{−/−})-deficient mice 8 to 10 weeks old were bred and maintained in conventional housing with constant light-dark

cycle (12 hour:12 hour) at the Animal Facility of the Department of Parasitology from the Institute of Biomedical Sciences at the University of São Paulo (ICB/USP). Mice received water and food of regular diet at ad libitum. *Nlrp3*^{−/−} and *Aim2*^{−/−} mice were provided by V. Dixit (Genentech, USA); *Asc*^{−/−}, *Casp1/11*^{−/−}, and *Nlr4*^{−/−} mice by R. Flavell (Yale University, USA); *Il1r1*^{−/−} mice by D. Zamboni (São Paulo University, Brazil); and *Il1b*^{−/−} mice by Y. Iwakura (Tokyo University of Science, Japan). At ICB/USP, *Nlrp3*^{−/−}, *Aim2*^{−/−}, and *Il1b*^{−/−} mice were kept under the responsibility of C.R.F.M. holding the material transfer agreements OM-502612, OM-214010, and M18-131, respectively. All experiments were performed in accordance with the ethical guidelines for experiments with mice, and all procedures were approved by the Animal Health Committee of the Institute of Biomedical Sciences of the University of São Paulo (CEUA no. 58/12fls128livro2). The guidelines for animal use and care were based on the standards established by the National Council for Control of Animal Experimentation (CONCEA).

Murine placental malaria

To obtain pregnant mice, two females 8 to 14 weeks of age were mated to one male of the same strain and age. Pregnancy was monitored as described elsewhere (11, 22). Briefly, the combination of vaginal plug and body weight measurement allowed the gestation time to be determined. G1 was defined in the day in which a vaginal plug was detected. Successful pregnancies were confirmed between G10 and G13 when females exhibited an average increase of 3 to 4 g in their body weight. On the other hand, unexpected weight loss was interpreted as an indicator of pregnancy complications or interruption.

At G13, pregnant mice were intravenously inoculated with 2×10^5 *Pb* NK65^{GFP} iRBCs obtained from frozen vials. *Pb* NK65^{GFP} (*Pb*) express constitutively green fluorescent protein (GFP) (40). G13 was determined as the optimal time point for the infection, as infection at an earlier stage would hamper the pregnancy term (22). At G19 (6 days after infection), parasitemia was analyzed; pregnant mice were euthanized and submitted to C-section. Then, placentas were collected, fetuses were weighed, and the number of resorptions and stillbirths were quantified. Four placentas from each pregnant mouse were collected, pooled, and stored at −80°C until use. Remaining placentas were separated in two; one-half was stored in RNeasy lysis buffer (Applied Biosystems, USA) for future protein or total RNA extraction. The other half was fixed in 10% (v/v) buffered formalin (Sigma-Aldrich, USA) for 48 hours, after which the material was stored in 70% ethanol until use. NI pregnant mice were used as controls. Parasitemia was determined using flow cytometry by quantifying GFP-iRBCs. Cell acquisition was done using the FACSCalibur cytometer (BD Biosciences, USA) and analyzed with “FlowJo 10.07r2” software (Treestar, Ashland, USA).

Anakinra treatment

C57BL/6 pregnant mice, infected and NI, were subcutaneously treated with Anakinra (100 mg/kg; Sobi, Germany), a recombinant of the IL-1Ra, for 5 days. Treatment started at G14 (24 hours after infection) and continued until G19 (12). Concomitantly, two additional control groups of pregnant mice, infected and NI, were treated with Anakinra (100 mg/kg) denaturated at 65°C in PBS (vehicle).

Morphometric analysis of murine placentas

Nonconsecutive placenta sections (5 μ m) were stained with H&E and examined using the Zeiss camera (AxioCamHRC) connected to

a Zeiss light microscope (AxioImager, M2). Morphometric analysis was done as previously described (9, 22). Briefly, vascular spaces were quantified in the analysis of placental sections stained with H&E. For each section, three areas of IVS were randomly selected for image acquisition ($\times 20$ magnification). Images were analyzed using ImageJ software. For the morphometric analysis, placenta sections were examined by different pathologists using the double-blind method.

Gene expression quantification

Total RNA was isolated and purified from 100 mg of placental tissue using the RNeasy Mini Kit (Qiagen, Germany) following the manufacturer's recommendations. One microgram of total RNA was converted into complementary DNA (cDNA) using the Transcriptor First cDNA Synthesis (Roche, Switzerland) with randomized hexamer primers. The expression of the genes *Slc38a1* (SNAT1), *Slc38a2* (SNAT2), and *Slc2a1* (GLUT1) was quantified using the Power SYBR Green PCR Master Mix (Thermo Fisher Scientific, USA). The cDNA of each gene was amplified using the following primers: *Slc38a1* (5'-GAGCAAGTCTTCGGCACCAC-3' and 5'-CACCATCACCACCAACACTCG-3'), *Slc38a2* (5'-GCGTTG-GCATTCAATAGC-3' and 5'-CGTTCATCATCCGCTCTCC-3'), and *Slc2a1* (5'-TGTGCTCATGACCATCG-3' and 5'-AAGGCCACAAAG-CCAAAGAT-3') (41, 42). The gene glyceraldehyde-3-phosphate dehydrogenase (GAPDH) (Hs99999905, Thermo Fisher Scientific, USA) was used as endogenous control, and each sample was normalized to the respective *Gapdh* expression. PCRs were performed in a 7500 Fast Real-Time PCR System (Thermo Fisher Scientific, USA), and relative quantification was calculated by the $\Delta\Delta C_t$ method.

Protein analysis

Fragments of NI and *Pf*-I human and NI and *Pb*-infected (*Pb*-I) mouse placentas preserved in RNAlater were analyzed (fig. S6). The placental fragments were macerated in radioimmunoprecipitation assay buffer containing a cocktail of protease inhibitors (10 μ l/ml) (Sigma-Aldrich, Germany) and incubated for 20 min on ice, followed by centrifugation to collect the protein extract contained in the supernatant. To analyze caspase-1 expression, total protein extract (30 μ g of each sample) of six NI and eight *Pf*-I human and four NI and five *Pb*-I mouse placentas was separated using a 15% SDS-polyacrylamide gel electrophoresis (SDS-PAGE) together with a molecular weight marker (Bio-Rad, USA), followed by transfer onto polyvinylidene difluoride (PVDF) membranes (Bio-Rad, USA) for 18 hours, 30 V at 4°C. Then, membranes were blocked with a 10% solution of skimmed milk for 2 hours at room temperature. Membranes were incubated with a primary antibody specific for the caspase-1 p20 subunit (G19) (Santa Cruz Biotechnology, USA) in murine placentas and a specific primary antibody anti-caspase-1 clone 5B10 (BioLegend, USA) in human placentas. After being washed three times with tris-buffered saline with tween (TBS-T), membranes were incubated with HRP-conjugated secondary goat antibody (Santa Cruz Biotechnology, USA). Data normalization was done using an anti- β -actin (Novus, USA) antibody at a concentration of 1:500,000. Every staining was revealed by chemiluminescence (Bio-Rad, USA), and images were acquired using the ChemiDoc XRS+ System camera (Bio-Rad, USA) and the ImageLab software (Bio-Rad, USA). To analyze the expression of AIM2, NLRP3, NLRP4, ASC, and IL-1R, equal amounts (25 μ g) of protein from each extract of five NI and five *Pf*-I human placentas were solubilized in a sample buffer [60 mM tris-HCl (pH 6.8), 2% SDS, 10% glycerol, and 0.01% bromophenol blue] and subjected to SDS-

PAGE (12%). Proteins were transferred to PVDF membranes, incubated with a blocking buffer solution (Thermo Fisher Scientific, USA) and 5% bovine serum albumin (1:1). Then, membranes were cut according to each protein molecular weight, and each segment of the membranes was incubated with the following antibodies: rabbit polyclonal anti-IL-1R (1:250; ab106278), mouse monoclonal anti-NLRP3 (1:500; ab106097), rabbit polyclonal anti-NLRP4 (1:500; ab115537), rabbit polyclonal anti-ASC (1:500; ab47092), and rabbit polyclonal anti-AIM2 (1:250; ab93015) (all from Abcam, UK) and with a mouse monoclonal anti- α -tubulin clone B-5-1-2 antibody (1:10,000; T5168; Sigma-Aldrich, USA) as a loading control. Membranes were then incubated with HRP-conjugated secondary antibody (Vector Laboratories, USA). Image acquisition was performed using the Alliance chemiluminescence detection system (UVITEC, UK). Quantitative densitometry was carried out using the ImageJ software (National Institutes of Health). The volume density of the chemiluminescent bands was calculated as integrated optical density \times mm² after background correction.

Cytokine quantification

To quantify the IL-1 β , TNF- α , IL-6, and IL-10 cytokines in human placental blood, the cytometric bead array (CBA) Human Inflammatory Cytokines Kit (BD Biosciences, USA) was used according to the manufacturer's instructions. For samples collected from mice placentas or culture supernatant, the cytokine IL-1 β was measured by enzyme-linked immunosorbent assay (BioLegend, USA), and IFN- γ , TNF- α , IL-6, and IL-10 were quantified by CBA using the Mouse Th1/Th2/Th17 Cytokine Kit (BD Biosciences, USA), as determined by the manufacturer. Bead acquisition was made using the FACSCalibur flow cytometer (BD Biosciences, USA), and the analysis was done by the FCAP 3.01 software (BD Biosciences, USA). Cytokine concentrations quantified in plasma or culture supernatants were expressed in picograms per milliliter. For macerates of placental tissue, cytokine concentrations were expressed as picograms (cytokine) per milligram (total protein).

Statistical analysis

Statistic differences between groups were tested by the one-way analysis of variance (ANOVA) with Bonferroni's correction or two-way ANOVA, Student's *t* test, Mann-Whitney, or chi-square. Spearman's rank-order nonparametric correlation test was applied to determine the association between studied variables. Tests were used according to each situation, as described in figure legends. Statistical tests were done using GraphPad Prism 5.0 (GraphPad Software, USA). *P* values ≤ 0.05 were considered statistically significant.

SUPPLEMENTARY MATERIALS

Supplementary material for this article is available at <http://advances.sciencemag.org/cgi/content/full/6/10/eaax6346/DC1>

Fig. S1. Heat map matrixes of Spearman's correlation coefficients between pregnancy and inflammatory parameters.

Fig. S2. Ablation of inflammasome components in mice does not impact peripheral parasitemia during pregnancy.

Fig. S3. IL-1 axis activation impairs nutrient transporters that are reverted by IL-1Ra.

Fig. S4. Absence of IL-1 β signaling restrains the increase in parasitemia during pregnancy.

Fig. S5. Ablation of Myd88 in infected pregnant mice improves pregnancy outcomes and impairs IL-1 β secretion.

Fig. S6. Western blotting original images.

Table S1. Baseline characteristics of mothers and newborns at delivery.

Table S2. Placental parameters of NI and infected pregnant women.

[View/request a protocol for this paper from Bio-protocol.](#)

REFERENCES AND NOTES

1. S. J. Rogerson, L. Hviid, P. E. Duffy, R. F. G. Leke, D. W. Taylor, Malaria in pregnancy: Pathogenesis and immunity. *Lancet Infect. Dis.* **7**, 105–117 (2007).
2. B. J. Brabin, C. Romagosa, S. Abdelgalil, C. Menéndez, F. H. Verhoeff, R. McGready, K. A. Fletcher, S. Owens, U. D'Alessandro, F. Nosten, P. R. Fischer, J. Ordi, The sick placenta-the role of malaria. *Placenta* **25**, 359–378 (2004).
3. A. Erlebacher, Immunology of the maternal-fetal interface. *Annu. Rev. Immunol.* **31**, 387–411 (2013).
4. V. M. Abrahams, The role of the Nod-like receptor family in trophoblast innate immune responses. *J. Reprod. Immunol.* **88**, 112–127 (2011).
5. V. M. Abrahams, G. Mor, Toll-like receptors and their role in the trophoblast. *Placenta* **26**, 540–547 (2005).
6. G. Krishnegowda, A. M. Hajjar, J. Zhu, E. J. Douglass, S. Uematsu, S. Akira, A. S. Woods, D. C. Gowda, Induction of proinflammatory responses in macrophages by the glycosylphosphatidylinositols of *Plasmodium falciparum*: Cell signaling receptors, glycosylphosphatidylinositol (GPI) structural requirement, and regulation of GPI activity. *J. Biol. Chem.* **280**, 8606–8616 (2005).
7. P. Parroche, F. N. Lauw, N. Goutagny, E. Latz, B. G. Monks, A. Visintin, K. A. Halmen, M. Lamphier, M. Olivier, D. C. Bartholomeu, R. T. Gazzinelli, D. T. Golenbock, Malaria hemozoin is immunologically inert but radically enhances innate responses by presenting malaria DNA to Toll-like receptor 9. *Proc. Natl. Acad. Sci.* **104**, 1919–1924 (2007).
8. N. Warner, G. Nuñez, MyD88: A critical adaptor protein in innate immunity signal transduction. *J. Immunol.* **190**, 3–4 (2013).
9. R. Barboza, A. S. Reis, L. G. da Silva, L. Hasenkamp, K. R. B. Pereira, N. O. S. Câmara, F. T. M. Costa, M. R. D. Lima, J. M. Alvarez, S. B. Boscardin, S. Epiphanyo, C. R. F. Marinho, MyD88 signaling is directly involved in the development of murine placental malaria. *Infect. Immun.* **82**, 830–838 (2014).
10. R. Barboza, F. A. Lima, A. S. Reis, O. J. Murillo, E. P. M. Peixoto, C. L. Bandeira, W. L. Fotoran, L. R. Sardinha, G. Wunderlich, E. Bevilacqua, M. R. D. Lima, J. M. Alvarez, F. T. M. Costa, L. A. Gonçalves, S. Epiphanyo, C. R. F. Marinho, TLR4-mediated placental pathology and pregnancy outcome in experimental malaria. *Sci. Rep.* **7**, 8623 (2017).
11. R. Barboza, L. Hasenkamp, A. Barateiro, O. Murillo, E. P. M. Peixoto, F. A. Lima, A. S. Reis, L. A. Gonçalves, S. Epiphanyo, C. R. F. Marinho, Fetal-derived MyD88 signaling contributes to poor pregnancy outcomes during gestational malaria. *Front. Microbiol.* **10**, 68 (2019).
12. M. A. Ataíde, W. A. Andrade, D. S. Zamboni, D. Wang, M. d. C. Souza, B. S. Franklin, S. Elian, F. S. Martins, D. Pereira, G. Reed, K. A. Fitzgerald, D. T. Golenbock, R. T. Gazzinelli, Malaria-induced NLRP12/NLRP3-dependent caspase-1 activation mediates inflammation and hypersensitivity to bacterial superinfection. *PLOS Pathog.* **10**, e1003885 (2014).
13. P. Broz, V. M. Dixit, Inflammasomes: Mechanism of assembly, regulation and signalling. *Nat. Rev. Immunol.* **16**, 407–420 (2016).
14. M. T. Shio, S. C. Eisenbarth, M. Savaria, A. F. Vinet, M. J. Bellemare, K. W. Harder, F. S. Suterwala, D. S. Bohle, A. Descoteaux, R. A. Flavell, M. Olivier, Malarial hemozoin activates the NLRP3 inflammasome through Lyn and Syk kinases. *PLOS Pathog.* **5**, e1000559 (2009).
15. P. Kalantari, R. B. DeOliveira, J. Chan, Y. Corbett, V. Rathinam, A. Stutz, E. Latz, R. T. Gazzinelli, D. T. Golenbock, K. A. Fitzgerald, Dual engagement of the NLRP3 and AIM2 inflammasomes by plasmodium-derived hemozoin and DNA during malaria. *Cell Rep.* **6**, 196–210 (2014).
16. M. J. Mulla, K. Myrtolli, J. Potter, C. Boeras, P. B. Kavathas, A. K. Sfakianaki, S. Tadesse, E. R. Norwitz, S. Guller, V. M. Abrahams, Uric acid induces trophoblast IL-1 β production via the inflammasome: Implications for the pathogenesis of preeclampsia. *Am. J. Reprod. Immunol.* **65**, 542–548 (2011).
17. J. Poovassery, J. M. Moore, Association of malaria-induced murine pregnancy failure with robust peripheral and placental cytokine responses. *Infect. Immun.* **77**, 4998–5006 (2009).
18. P. Boeuf, E. H. Aitken, U. Chandrasiri, C. L. L. Chua, B. McInerney, L. McQuade, M. Duffy, M. Molyneux, G. Brown, J. Glazier, S. J. Rogerson, Plasmodium falciparum malaria elicits inflammatory responses that dysregulate placental amino acid transport. *PLOS Pathog.* **9**, e1003153 (2013).
19. C. T. Berger, M. Recher, U. Steiner, T. M. Hauser, A patient's wish: Anakinra in pregnancy. *Ann. Rheum. Dis.* **68**, 1794–1795 (2009).
20. D. E. Furst, Anakinra: Review of recombinant human interleukin-1 receptor antagonist in the treatment of rheumatoid arthritis. *Clin. Ther.* **26**, 1960–1975 (2004).
21. P. B. Kavathas, C. M. Boeras, M. J. Mulla, V. M. Abrahams, Nod1, but not the ASC inflammasome, contributes to induction of IL-1 β secretion in human trophoblasts after sensing of *Chlamydia trachomatis*. *Mucosal Immunol.* **6**, 235–243 (2013).
22. R. Neres, C. R. F. Marinho, L. A. Gonçalves, M. B. Catarino, C. Penha-Gonçalves, Pregnancy outcome and placenta pathology in *Plasmodium berghei* ANKA infected mice reproduce the pathogenesis of severe malaria in pregnant women. *PLOS ONE* **3**, e1608 (2008).
23. G. Lopez-Castejon, D. Brough, Understanding the mechanism of IL-1 β secretion. *Cytokine Growth Factor Rev.* **22**, 189–195 (2011).
24. A. M. Moormann, A. D. Sullivan, R. A. Rochford, S. W. Chensue, P. J. Bock, T. Nyirenda, S. R. Meshnick, Malaria and pregnancy: Placental cytokine expression and its relationship to intrauterine growth retardation. *J. Infect. Dis.* **180**, 1987–1993 (1999).
25. M. Marzi, A. Viganò, D. Trabattini, M. L. Villa, A. Salvaggio, E. Clerici, M. Clerici, Characterization of type 1 and type 2 cytokine production profile in physiologic and pathologic human pregnancy. *Clin. Exp. Immunol.* **106**, 127–133 (1996).
26. J. Poovassery, J. M. Moore, Murine malaria infection induces fetal loss associated with accumulation of *Plasmodium chabaudi* AS-infected erythrocytes in the placenta. *Infect. Immun.* **74**, 2839–2848 (2006).
27. J. Yui, M. Garcia-Lloret, T. G. Wegmann, L. J. Guilbert, Cytotoxicity of tumour necrosis factor- α and gamma-interferon against primary human placental trophoblasts. *Placenta* **15**, 819–835 (1994).
28. B. S. Franklin, P. Parroche, M. A. Ataíde, F. Lauw, C. Ropert, R. B. de Oliveira, D. Pereira, M. S. Tada, P. Nogueira, L. H. P. da Silva, H. Bjorkbacka, D. T. Golenbock, R. T. Gazzinelli, Malaria primes the innate immune response due to interferon- γ induced enhancement of toll-like receptor expression and function. *Proc. Natl. Acad. Sci. U.S.A.* **106**, 5789–5794 (2009).
29. E. Latz, T. S. Xiao, A. Stutz, Activation and regulation of the inflammasomes. *Nat. Rev. Immunol.* **13**, 397–411 (2013).
30. N. W. Lucchi, D. S. Peterson, J. M. Moore, Immunologic activation of human syncytiotrophoblast by *Plasmodium falciparum*. *Malar. J.* **7**, 42 (2008).
31. C. L. L. Chua, G. Brown, J. A. Hamilton, S. Rogerson, P. Boeuf, Monocytes and macrophages in malaria: Protection or pathology? *Trends Parasitol.* **29**, 26–34 (2013).
32. W. Li, Y. Chang, S. Liang, Z. Zhong, X. Li, J. Wen, Y. Zhang, J. Zhang, L. Wang, H. Lin, X. Cao, H. Huang, F. Zhong, NLRP3 inflammasome activation contributes to Listeria monocytogenes-induced animal pregnancy failure. *BMC Vet. Res.* **12**, 36 (2016).
33. U. P. Chandrasiri, C. L. L. Chua, A. J. Umbers, E. Chaluluka, J. D. Glazier, S. J. Rogerson, P. Boeuf, Insight into the pathogenesis of fetal growth restriction in placental malaria: Decreased placental glucose transporter isoform 1 expression. *J. Infect. Dis.* **209**, 1663–1667 (2014).
34. J. G. Dombrowski, R. M. Souza, F. A. Lima, C. L. Bandeira, O. Murillo, D. d. S. Costa, E. P. M. Peixoto, M. d. P. Cunha, P. M. d. A. Zanotto, E. Bevilacqua, M. A. G. Grisotto, A. C. Pedrosa de Lima, J. d. M. Singer, S. Campino, T. G. Clark, S. Epiphanyo, L. A. Gonçalves, C. R. F. Marinho, Association of malaria infection during pregnancy with head circumference of newborns in the Brazilian Amazon. *JAMA Netw. Open* **2**, e193300 (2019).
35. N. W. Lucchi, J. Narayanan, M. A. Karell, M. Xayavong, S. Kariuki, A. J. DaSilva, V. Hill, V. Udhayakumar, Molecular diagnosis of malaria by photo-induced electron transfer fluorogenic primers: PET-PCR. *PLOS ONE* **8**, e56677 (2013).
36. Departamento de Vigilância Epidemiológica, Secretaria de Vigilância em Saúde, *Guia prática de tratamento da malária no Brasil*. (Brasília: Ministério da Saúde, ed. 1, 2010).
37. J. Kononen, L. Bubendorf, A. Kallioniemi, M. Bärland, P. Schraml, S. Leighton, J. Torhorst, M. J. Mihatsch, G. Sauter, O.-P. Kallioniemi, Tissue microarrays for high-throughput molecular profiling of tumor specimens. *Nat. Med.* **4**, 844–847 (1998).
38. R. M. Souza, R. Ataíde, J. G. Dombrowski, V. Ippólito, E. H. Aitken, S. N. Valle, J. M. Alvarez, S. Epiphanyo, C. R. F. Marinho, Placental histopathological changes associated with *Plasmodium vivax* infection during pregnancy. *PLOS Negl. Trop. Dis.* **7**, e2071 (2013).
39. H. J. Kliman, J. E. Nestler, E. Sermasi, J. M. Sanger, J. F. Strauss III, Purification, characterization, and in vitro differentiation of cytotrophoblasts from human term placenta. *Endocrinology* **118**, 1567–1582 (1986).
40. A. A. Sultan, V. Thathy, V. Nussenzweig, R. Ménard, Green fluorescent protein as a marker in *Plasmodium berghei* transformation. *Infect. Immun.* **67**, 2602–2606 (1999).
41. H. N. Jones, T. Crombleholme, M. Habli, Adenoviral-mediated placental gene transfer of IGF-1 corrects placental insufficiency via enhanced placental glucose transport mechanisms. *PLOS ONE* **8**, e74632 (2013).
42. L. C. Kusinski, J. L. Stanley, M. R. Dilworth, C. J. Hirt, I. J. Andersson, L. J. Renshall, B. C. Baker, P. N. Baker, C. P. Sibley, M. Wareing, J. D. Glazier, eNOS knockout mouse as a model of fetal growth restriction with an impaired uterine artery function and placental transport phenotype. *Am. J. Physiol. Regul. Integr. Comp. Physiol.* **303**, R86–R93 (2012).

Acknowledgments: We thank B. Paulo Albe from the Institute of Biomedical Sciences of the University of São Paulo for technical assistance and C. Ferreira do Nascimento from AC Camargo Hospital for technical assistance with the tissue microarray technique. We also thank the nurses and technicians of the Hospital da Mulher e da Criança do Juruá and the Gerência de Endemias/SESACRE team for their invaluable assistance. We are grateful to V. Dixit (Genentech, USA) for providing the *Nlrp3*^{-/-} and *Aim2*^{-/-} mice; R. Flavell (Yale University, USA) for providing the *Asc*^{-/-}, *Casp1/11*^{-/-}, and *Nlr4*^{-/-} mice; D. Zamboni (São Paulo University, Brazil) for providing the *Il1r*^{-/-} mice; and Y. Iwakura (Tokyo University of Science, Japan) for providing the *Il1b*^{-/-} mice. **Funding:** This work was primarily funded by the São Paulo Research Foundation—FAPESP (grant nos. 2014/09964-5, 2016/07030-0, and 2018/20468-0 to C.R.F.M.; 2014/20451-0 and 2017/05782-8 to S.E.; 2012/16525-2 to F.M.T.C.; 2015/23395-6 and

2015/50650-7 to A.P.; and 2013/0729-4 to L.L.), the Brazilian National Council for Scientific and Technological Development–CNPq (grant nos. 475771/2009-5 to C.R.F.M. and 455863/2014-8 to S.E.), and Maranhão Research Foundation–FAPEMA (grant 129790/2015 to A.S.R.). A.S.R., O.M., F.A.L., A.B., J.D., R.B., and L.A.G. were supported by fellowships from FAPESP (2011/19048-8, 2013/00981-1, 2013/16417-8, 2017/03939-7, 2012/04755-3, 2011/17880-8, and 2015/06106-0, respectively). The funders had no role in the analysis design, data collection, analysis, decision to publish, and preparation of the manuscript. **Author contributions:** A.S.R. designed, performed, and analyzed all the experiments and drafted the manuscript. R.B., O.M., A.B., E.P.M.P., F.A.L., V.M.G., J.G.D., V.N.C.L., F.A., C.L.B., R.B.D.A., R.N., and R.M.S. helped design, perform, and analyze the experiments and discussed the hypotheses. F.T.M.C., A.P., E.B., C.W., G.W., G.P., L.L., K.R.B., and S.E. helped in data interpretation and analysis and discussed the hypotheses. C.P.-G. and L.A.G. helped in data interpretation and analysis, discussed the hypotheses, and helped draft the manuscript. C.R.F.M. designed and supervised the project, provided funding for all experiments, helped in data interpretation and analysis, and drafted the manuscript. All authors reviewed and approved the manuscript. **Competing interests:** The authors declare that they have no competing interests. **Data and materials availability:** All data needed to evaluate the conclusions in the paper are present in the paper and/or the Supplementary Materials. Additional data related to this paper may be requested from the

authors. The *Nlrp3*^{−/−} and *Aim2*^{−/−} mice can be provided by Genentech pending scientific review and a completed material transfer agreement. Requests for the *Nlrp3*^{−/−} and *Aim2*^{−/−} mice should be submitted to www.gene.com/scientists/mta. The *Il1b*^{−/−} mice can be provided by Tokyo University of Science (Japan) pending scientific review and a completed material transfer agreement. Requests for the *Il1b*^{−/−} mice should be submitted to www.rs.tus.ac.jp/iwakuralab/en/resource.html.

Submitted 9 April 2019

Accepted 11 December 2019

Published 4 March 2020

10.1126/sciadv.aax6346

Citation: A. S. Reis, R. Barboza, O. Murillo, A. Barateiro, E. P. M. Peixoto, F. A. Lima, V. M. Gomes, J. G. Dombrowski, V. N. C. Leal, F. Araujo, C. L. Bandeira, R. B. D. Araujo, R. Neres, R. M. Souza, F. T. M. Costa, A. Pontillo, E. Bevilacqua, C. Wrenger, G. Wunderlich, G. Palmisano, L. Labriola, K. R. Bortoluci, C. Penha-Gonçalves, L. A. Gonçalves, S. Epiphany, C. R. F. Marinho, Inflammatory activation and IL-1 signaling during placental malaria induce poor pregnancy outcomes. *Sci. Adv.* **6**, eaax6346 (2020).